Incremental Learning of Traversability Cost for Aerial Reconnaissance Support to Ground Units

Miloš Prágr[0000−0002−8213−893X], Petr Čížek[0000−0001−6722−3928], and Jan Faigl[0000−0002−6193−0792]

Faculty of Electrical Engineering, Czech Technical University in Prague,
Technicka 2, 166 27, Prague, Czech Republic
{pragrmi1,cizekpe6,faiglj}@fel.cvut.cz
https://comrob.fel.cvut.cz

Abstract. In this paper, we address traversability cost estimation using exteroceptive and proprioceptive data collected by a team of aerial and ground vehicles. The main idea of the proposed approach is to estimate the terrain traversability cost based on the real experience of the multi-legged walking robot with traversing different terrain types. We propose to combine visual features with the real measured traversability cost based on proprioceptive signals of the utilized hexapod walking robot as a ground unit. The estimated traversability cost is augmented by extracted visual features from the onboard robot camera, and the features are utilized to extrapolate the learned traversability model for an aerial scan of new environments to assess their traversability cost. The extrapolated traversability cost can be utilized in the high-level mission planning to avoid areas that are difficult to traverse but not visited by the ground units. The proposed approach has been experimentally verified with a real hexapod walking robot in indoor and outdoor scenarios.

1 Introduction

Robots deployed in remote missions such as extraterrestrial exploration [5] have to deal with challenges related to the traversability of the operational area to efficiently accomplish the mission and avoid hard-to-traverse regions that might impose risks to the robotic platform. Various robotic systems suitable for different terrain types are emerging, with multi-legged walking robots being already deployed in several scenarios, e.g., search and rescue tasks [18], inspection of the failed Fukushima nuclear power plant [6], and underwater marine operations [10]. Therefore, we consider a hexapod walking robot as a suitable ground robot that is capable of traversing complex terrains, especially when aided by an efficient locomotion control such as [13]. However, it is still beneficial to further increase mission efficiency by planning to avoid hard-to-traverse areas that can be assessed using a cost of transport characterizing the terrain traversability.

In autonomous missions, terrains may not be a priory known, and therefore, the robots have to learn the terrain traversability model incrementally to immediately assess the traversed terrain and extrapolate the assessment for the

forthcoming areas. Such a model can be based on the terrain classification into discrete classes [15], but it can also be a continuous measure based on exteroceptive [19] or proprioceptive data [11]. The fundamental requirement of the traversability model suitable for a high-level mission planning is the ability to extrapolate the learned traversability estimation to not visited but already seen areas, e.g., by utilizing Unmanned Aerial Vehicle (UAV) to efficiently explore the environment and evaluate its cost of transport using a ground walking robot. Such a system of cooperative navigation of a UAV and a legged robot is proposed in [7]; however, the authors based the traversability estimation on fixed local terrain characteristics, which deny the robot exploitation of newly collected information about the terrain traversability.

In this paper, we report on the deployment of learning framework [17] for the cost of transport regression from RGB-D data that allows combining numerous learning algorithms and terrain characterization features to learn and infer the traversability cost. However, we consider the Fast Incremental Gaussian Mixture Network (F-IGMN) [16], an online incremental Gaussian mixture algorithm, and a set of computationally efficient point cloud-based terrain descriptors for the herein presented results of the practical deployment of the framework. The descriptors are robust to viewpoint changes, and they can be captured both from the robot near-to-ground viewpoint and also from the aerial viewpoint.

The rest of the paper is organized as follows. The most related existing approaches and the utilized cost of transport are presented in the next section. The addressed problem is described in Section 3 and a brief overview of the used learning framework for the regression of the cost of transport is presented in Section 4. The main part of the paper is a report on the experimental deployment and achieved results for both indoor and outdoor scenarios that are reported in Section 5. Concluding remarks are dedicated to Section 6.

2 Related work

Approaches that tackle the problem of the terrain traversability characterization can be divided into two main categories. The first category consists of methods utilizing classification to a discrete set of classes. These classes can be either human-observed terrain types [4, 12, 15] (e.g., grass, rock, sand, etc.), or simple binary distinction between passable/impassable terrains [19]. Three terrain classes for the simulated Martian terrain are considered in [15] but the passable-impassable distinction is utilized in [19]. The authors of [4, 12] combine broader sets of classes with an impassable or otherwise undesirable obstacle class.

The second category characterizes the traversed terrains with a continuous function. Approaches that use proprioceptive [11], or exteroceptive [3, 19] data can be further distinguished. Continuous traversability assessment functions can be utilized as a motion cost in planning algorithms. In [3] and [19], assessment functions based directly on locally observed properties are presented. Two-level discrete-continuous functions using three hazard criteria (i.e., slope, roughness, and step height) are proposed in [19]. A set of general global features is used to

define the terrain traversability for a large wheeled vehicle in [3]. The utilized descriptors are the position, density, and point cloud distributions of the sensed obstacles. The main disadvantage of these approaches is that the traversability value assigned to a specific terrain cannot be directly updated based on the new robot experience.

In proprioceptive approaches such as the Cost of Transport (CoT) [20], the terrain traversability property is inferred from the terrain traversal experience. A particular value of the CoT is proportional to the energy consumed for traversing the respective terrain and to the inverse of the traversal speed. The CoT for battery powered robots is defined in [11] as

$$\mathrm{CoT} = \frac{1}{m \cdot g} \cdot \frac{P_{\mathrm{inst}}}{v}, \tag{1}$$

where m is the robot weight, g is the gravitational acceleration, v is the robot speed, and P_{inst} is the instantaneous power consumption computed from the battery voltage V and the instantaneous current I_{inst} drawn from the battery

$$P_{\mathrm{inst}} = V \cdot I_{\mathrm{inst}}. \tag{2}$$

Proprioceptive-based approaches and discrete terrain classification approaches need to be paired with terrain characterization features to enable terrain evaluation from a distance. Simple color space features as a part of the respective terrain descriptors are used in [1, 2, 15]. Color- and reflectance-based vegetation indexes have been used in [4, 21]. The Gabor filter response combined with the HSV and grayscale descriptors are used as features on aerial images in [3].

Among the various shape and geometric features reported in [2, 9, 12, 19], the most notable is the fact that all approaches use some height-based descriptor. It requires a selection of the canonical vertical orientation, which may be difficult, e.g., when dealing with sloped mountain terrains. The Principal Component Analysis (PCA) to characterize the terrain shape is utilized in [22] that is further combined with the normal vector based statistics in [12].

A simple feature set consisting of the height feature and histograms in the HSV color space is proposed in [2]. A set of seven geometric features extracted from a point cloud constructed using a stereo camera is utilized to characterize the terrain roughness and step height in [9]. Voxel, point cloud, and color features are used for terrain and vegetation classification by the authors of [4]. Their descriptors include scan line features, a vegetation index, and the PCA.

Based on the literature review briefly reported in this section, and also based on our results [17], we have selected the CoT terrain traversability measure [11] as the traversability assessment function that is combined with the computationally inexpensive color-geometric features.

3 Problem statement

The problem addressed in this paper is a remote estimation of the CoT defined by (1). The requested model of the CoT is learned using our incremental learning

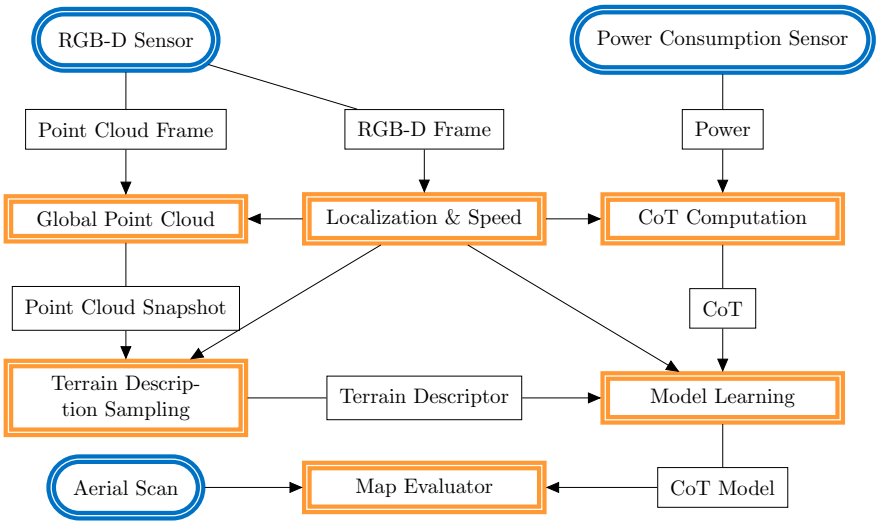

Fig. 1. Individual building blocks of the CoT regression framework [17].

framework [17] for the CoT regression of a priory unknown terrains by a hexapod walking robot that collects real measurements of the terrain traversability using RGB-D images and robot power consumption readings.

The learned traversability model is utilized for the evaluation of environment scans, which can be captured from a viewpoint that differs from the robot near-to-ground position, e.g., by a UAV. Hence, we aim for a two-agent setup, where the ground walking robot learns and creates the terrain traversability model and the UAV can evaluate the environment terrains remotely. Moreover, we consider that the ground robot incrementally learns the terrain traversability property and provides continuously improving the traversability assessment.

4 Incremental Traversability Learning Framework

The herein presented results leverage on the CoT regression framework introduced in [17], which is schematically shown in Fig. 1. The framework can run online, and its building blocks are as follows.

RGB-D sensor provides RGB and depth images with 30 frames per second. For each RGB-D frame, an individual colored point cloud is created.

Localization & Speed localizes the robot and the captured RGB-D frames using the ORB-SLAM [14]. Besides, it allows to compute the speed of the robot utilized in the calculation of the CoT according to $v = ds/dt$, where ds is the measured robot displacement for the fixed period $dt = 20$ s.

Global point cloud is created by merging the individual localized point clouds with the frequency approx. 1 Hz. Its size is limited to 2M points, whereas the

individual point clouds consist roughly of 300k points. Point cloud snapshots are further down-sampled to 5–15k points. Note, the externally supplied aerial environment scan is constructed similarly.

Power consumption sensor provides mean power consumption using moving average with 10 s long window of instantaneous power readings calculated according to (2) from the raw battery voltage and current measured with the frequency 500 Hz.

CoT is computed from the robot velocity, the corresponding power consumption, and known robot weight and gravitational acceleration according to (1).

Terrain descriptors are computed at randomly sampled interest points in the robot field of view, i.e., points that are likely to be traversed soon. For each processed robot position, i.e., the localized frame, 30 points are selected. The Lab channel mean values in the 0.3 m radius neighborhood of the sampled point and the PCA shape feature [12], based on the 0.2 m radius neighborhood, are computed using the point cloud snapshot.

CoT regression model is learned from the CoT of the traversed terrain and terrain descriptors in the robot field of view. Therefore, the descriptors must be stored until the robot passes the respective locations. The stored descriptors are randomly pruned, and only the locations in front of the robot are kept for an extended period. An online incremental Gaussian mixture model called the Fast Incremental Gaussian Mixture Network (F-IGMN) [16] is utilized for learning and regression. In the F-IGMN, a single data point is processed in $\mathcal{O}(kd^2)$ for k components and d dimensions. The particular parametrization of the F-IGMN is $k = 10$ components, grace period $v_{\min} = 100$, minimal accumulated posterior $sp_{\min} = 3$, and scaling factor $\delta = 1$ with $d = 7 + 1$ dimensional CoT annotated terrain descriptor.

Map evaluator evaluates an externally provided point cloud using the CoT regression model. The point cloud is centered to $[0, 0, 0]$, and the global ground plane is fitted using the RANSAC scheme [8]. In such a way, the 0.1 m spaced grid of the 2D cost map can be constructed, which is then utilized for the grid-based path planning.

5 Experimental Results

The incremental learning framework [17] has been deployed and experimentally verified in three testing scenarios using battery-powered hexapod robot shown in Fig. 2a. The robot has six legs, each with three joints actuated by the Dynamixel AX-12A servomotors. Thus the robot has 18 controllable actuators, and it is capable of traversing irregular terrains using an adaptive motion gait [13], which utilizes only the position feedback from the servomotors. The robot is equipped with the Intel RealSense D435 RGB-D camera mounted approx. 15 cm above the ground and slightly skewed towards the ground to collect exteroceptive measurements and support localization and map building.

The regression framework overviewed in Section 4 is employed in the traversability cost assessment that is used in the grid-based path planning. Moreover, the

extrapolation of the learned CoT using features from exteroceptive measurements enables path planning for terrains not visited by the ground robot, but for which an aerial scan is available. In the experimental evaluation, an initial model of the real robot CoT is learned in an indoor setup first, and it is then evaluated in a testing setup that is reported in Section 5.1 and Section 5.2, respectively. In Section 5.3, we report on the performed outdoor deployment.

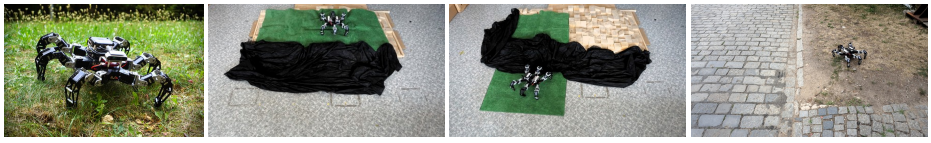

(a) Robot (b) Indoor Learning (c) Indoor Testing (d) Outdoor

Fig. 2. The (a) hexapod walking robot and the (b–d) three experimental setups.

5.1 Indoor Learning Setup

In the first evaluation scenario, the robot is remotely guided over three artificial indoor terrains, see Fig. 2b. First, the robot traverses over variable height and slope 10×10 cm wooden bricks covered by an artificial turf, which is firm enough to support the robot even if some of its legs are not directly supported by the bricks. After leaving the artificial turf, the robot continues over flat PVC flooring where it crawls in one direction, and then, it turns around and returns. Finally, the last terrain type is a flat ground covered by slippery black fabric.

The robot is guided by a human operator over the individual terrains who adjusts the robot speed to prevent it from getting stuck. Therefore, based on the experience from [17], the operator chooses the most efficient motion, the CoT is minimized, and we consider its measured values to be the ground truth. In this setup, the artificial turf is the hardest terrain to traverse, and the robot is guided slowly. The fastest locomotion is over the flat PVC flooring, but the overall speed is hindered by the turn. The flat ground covered by the black fabric allows medium speed because the fabric is slippery.

The aerial scan of the track is captured by manually scanning the track from 2 m above the terrain. The scan is evaluated using the CoT model altogether four times: (1) at the beginning of the experiment; after traversing (2) the artificial turf; (3) flat PVC flooring; and (4) the black fabric. Each time the model encompasses the robot experience up to the given instant. For each case, the CoT annotation of the scan is created, and a path over the experimental track is computed using the 8-neighborhood A*. The edge cost is defined as the mean CoT of the edge incident nodes, and the minimal observed CoT is utilized as a multiplier of the Euclidean heuristic. The start and goal locations are situated in such a way that the shortest path leads over the hard-to-traverse turf, the longest over the flat ground, and the mid-length path over the black fabric. The aerial scan annotations and the respective paths are shown in Fig. 3.

Naturally, the robot learns the traversability after it traverses the terrain. Therefore, the shortest path over the rough terrain is computed first and then

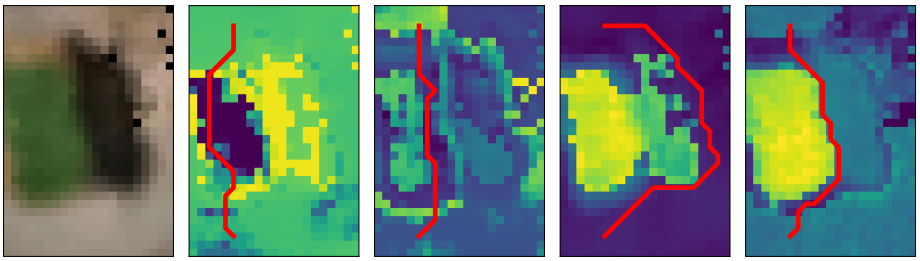

(a) Grid (b) Initial (c) After turf (d) After flat (e) After fabric

Fig. 3. Indoor learning scenario: the (a) 0.1 m sized cell grid over an aerial scan and its (b–e) CoT annotations with the planned path over the track. The used annotations correspond to four models sampled (b) at the beginning of the run; after traversing (c) the artificial turf; then after (d) the flat PVC flooring; (e) and finally the black fabric.

it is updated after observing both the rough and flat terrains. Besides, it can be noticed that the path planner avoids the black areas before traversing them.

5.2 Indoor Testing Setup

The model learned in the indoor learning setup has been utilized on a different indoor track shown in Fig. 2c. The track consists of the turf-covered bricks, flat PVC floor, and black fabric covered floor that all have been used in the learning setup. Besides, three additional (not previously utilized) terrains are used: the turf-covered floor, fabric covered bricks, and exposed bricks.

The same evaluation methodology as in the previous setup has been utilized, and individual evaluations of the aerial scan are visualized in Fig. 4. We found out that the terrains not be presented in the learning phase appear to be evaluated correctly, and the turf over the bricks is considered to be the most costly terrain type in the final evaluation. Further, the flat terrain is learned to be the cheapest terrain, and the fabric and bare cubes have a medium value of the CoT. Even though there is only a limited difference between the CoT over the fabric covered flooring and covered bricks, the shortest path is found over the flat ground.

5.3 Outdoor Setup

Two terrain types, which are less distinctive than the indoor terrains, have been considered in the outdoor experimental setup, see Fig. 2d. In this setup, the robot traverses over grass first, where the area is relatively scorched, and thus being a mix of green grass, yellow grass, and brown dirt. Then, the robot traverses stone brick pavement. Due to nearby construction work, the gray pavement is partially covered with dirt.

Similarly to the indoor learning setup, the CoT model is learned based on the measurements collected by the robot while traversing the outdoor track. Moreover, the final indoor model is also tested on the outdoor track. Individual

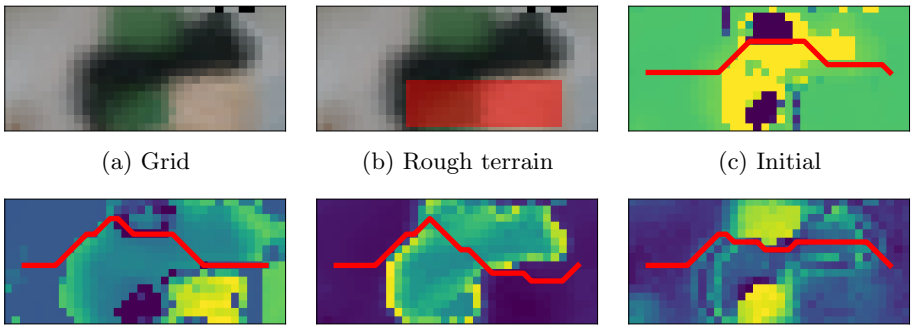

(a) Grid (b) Rough terrain (c) Initial

(d) After turf (e) After flat (f) After fabric

Fig. 4. Indoor testing scenario: the (a) 0.1 m sized cell grid over an aerial scan with the (b) rough terrain highlighted and its (c–f) CoT annotations with the planned path over the track. The used annotations correspond to the four models sampled (c) at the beginning of the run; after traversing (d) the artificial turf; (e) the flat PVC flooring; (f) and the black fabric.

evaluations of the aerial scan are depicted in Fig. 5. Again, the correct terrain evaluation is available only after the respective terrain type is traversed. In the initial model, the dirt/grass area is sharply distinguished from the pavement. However, the robot observes that the scorched grass and the pavement have a similar value of the CoT in the final model. It is correct and expected behavior as both terrains are relatively smooth and provide enough support. Overall, we found out that the indoor learned model performed surprisingly well when utilized on the outdoor dataset.

6 Conclusion

In this paper, we report on the deployment of the terrain traversability regression framework in practical indoor and outdoor setups. The framework infers a model of the CoT that can be extrapolated for aerial scans to build a cost map that is then utilized in path planning. Based on the reported results, the framework has been successfully evaluated, and it is a vital building block for further development. In particular, we aim to introduce an active perception into the presented framework to deliberately plan paths that will improve the model of the terrain traversability property.

Acknowledgements. This work has been supported by the Czech Science Foundation (GAČR) under research Project No. 18-18858S.

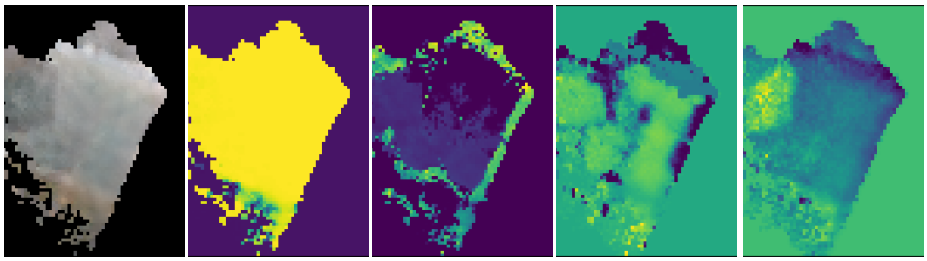

(a) Grid (b) Initial (c) After grass (d) After road (e) Indoor model

Fig. 5. Outdoor scenario: the (a) 0.1 m sized cell grid over an aerial scan and its (b–e) CoT annotations. The used annotations correspond to three models sampled (b) at the beginning of the run; after traversing (c) the grass and (d) the pavement. The annotation of the outdoor track using the indoor model from Section 5.1. A different behavior of the individual models can be observed when encountering areas not represented in the scan that are shown as the black areas in the grid image.

References

1. Bartoszyk, S., Kasprzak, P., Belter, D.: Terrain-aware motion planning for a walking robot. In: RoMoCo. pp. 29–34 (2017)
2. Belter, D., Wietrzykowski, J., Skrzypczynski, P.: Employing Natural Terrain Semantics in Motion Planning for a Multi-Legged Robot. Journal of Intelligent & Robotic Systems pp. 1–21 (2018)
3. Boris, S., Lin, E., Bagnell, J.A., Cole, J., Vandapel, N., Stentz, A.: Improving Robot Navigation Through Self-Supervised Online Learning. Journal of Field Robotics **23**(11-12), 1059–1075 (2006)
4. Bradley, D.M., Chang, J.K., Silver, D., Powers, M., Herman, H., Rander, P.: Scene Understanding for a High-mobility Walking Robot. In: IEEE/RSJ International Conference on Intelligent Robots and Systems (IROS). pp. 1144–1151 (2015)
5. Brown, D., Webster, G.: Now a stationary research platform, nasa's mars rover spirit starts a new chapter in red planet scientific studies. NASA Press Release (2010)
6. Falconer, J.: Toshiba unveils four-legged nuclear plant inspection robot. Innovation Toronto (2012), `http://www.innovationtoronto.com/2012/11/toshiba-unveils-four-legged-nuclear-plant-inspection-robot/`, [Accessed April 10, 2018]
7. Fankhauser, P., Bloesch, M., Krüsi, P., Diethelm, R., Wermelinger, M., Schneider, T., Dymczyk, M., Hutter, M., Siegwart, R.: Collaborative navigation for flying and walking robots. In: IEEE/RSJ International Conference on Intelligent Robots and Systems (IROS). pp. 2859–2866 (2016)
8. Fischler, M.A., Bolles, R.C.: Random sample consensus: A paradigm for model fitting with applications to image analysis and automated cartography. Communications of the ACM **24**(6), 381–395 (1981)
9. Homberger, T., Bjelonic, M., Kottege, N., Borges, P.V.K.: Terrain-dependant Control of Hexapod Robots using Vision. In: International Symposium on Experimental Robotics. pp. 92–102 (2016)

10. Jun, B.H., Shim, H., Kim, B., Park, J.Y., Baek, H., Yoo, S., Lee, P.M.: Development of seabed walking robot CR200. In: OCEANS MTS/IEEE Bergen: The Challenges of the Northern Dimension (2013)
11. Kottege, N., Parkinson, C., Moghadam, P., Elfes, A., Singh, S.P.: Energetics-informed hexapod gait transitions across terrains. In: IEEE International Conference on Robotics and Automation (ICRA). pp. 5140–5147 (2015)
12. Kragh, M., Jörgensen, R.N., Pedersen, H.: Object Detection and Terrain Classification in Agricultural Fields Using 3D Lidar Data. In: ICVS. pp. 188–197 (2015)
13. Mrva, J., Faigl, J.: Tactile sensing with servo drives feedback only for blind hexapod walking robot. In: RoMoCo. pp. 240–245 (2015)
14. Mur-Artal, R., Tardós, J.D.: ORB-SLAM2: An open-source SLAM system for monocular, stereo, and RGB-D cameras. IEEE Transactions on Robotics **33**(5), 1255–1262 (2017)
15. Otsu, K., Ono, M., Fuchs, T.J., Baldwin, I., Kubota, T.: Autonomous Terrain Classification with Co- and Self-Training Approach. Robotics and Automation Letters pp. 1–6 (2016)
16. Pinto, R.C., Engel, P.M.: A Fast Incremental Gaussian Mixture Model. PLoS ONE **10**(10), e0139931+ (2015)
17. Prágr, M., Čížek, P., Faigl, J.: Cost of Transport Estimation for Legged Robot Based on Terrain Features Inference from Aerial Scan. In: IEEE/RSJ International Conference on Intelligent Robots and Systems (IROS). pp. 1745–1750 (2018)
18. Roennau, A., Heppner, G., Nowicki, M., Dillmann, R.: LAURON V : A Versatile Six - Legged Walking Robot with Advanced Maneuverability. In: AIM. pp. 82–87 (2014)
19. Stelzer, A., Hirschmüller, H., Görner, M.: Stereo-vision-based navigation of a six-legged walking robot in unknown rough terrain. The International Journal of Robotics Research **31**(4), 381–402 (2012)
20. Tucker, V.A.: The Energetic Cost of Moving About: walking and running are extremely inefficient forms of locomotion. Much greater efficiency is achieved by birds, fish and bicyclists. American Scientist **63**(4), 413–419 (1975)
21. Ünsalam, C., Boyer, K., Anonymous: Linearized vegetation indices based on a formal statistical framework. IEEE Transactions on Geoscience and Remote Sensing **42**(7), 1575–1585 (2004)
22. Wellington, C., Stentz, A.: Online Adaptive Rough-Terrain Navigation in Vegetation. In: IEEE International Conference on Robotics and Automation (ICRA). pp. 96–101 (2004)